UNIVERSITY OF AMSTERDAM

UvA-DARE (Digital Academic Repository)

Half-precessional dynamics of monsoon rainfall near the East African Equator

Verschuren, D.; Sinninghe Damsté, J.S.; Moernaut, J.; Kristen, I.; Blaauw, M.; Fagot, M.; Haug, H.G.; van Geel, B.; De Batist, M.; Barker, P.; Vuille, M.; Conley, D.J.; Olago, D.O.; Milne, I.; Plessen, B.; Eggermont, H.; Wolff, C.; Hurrell, E.; Ossebaar, J.; Lyaruu, A.; van der Plicht, J.; Cumming, B.F.; Brauer, A.; Rucina, S.M.; Russell, J.M.; Keppens, E.; Hus, J.; Bradley, R.S.; Leng, M.; Mingram, J.; Nowaczyk, N.R.

DOI
10.1038/nature08520

Publication date
2009

Document Version
Final published version

Published in
Nature

Link to publication

Citation for published version (APA):
Verschuren, D., Sinninghe Damsté, J. S., Moernaut, J., Kristen, I., Blaauw, M., Fagot, M., Haug, H. G., van Geel, B., De Batist, M., Barker, P., Vuille, M., Conley, D. J., Olago, D. O., Milne, I., Plessen, B., Eggermont, H., Wolff, C., Hurrell, E., Ossebaar, J., ... Nowaczyk, N. R. (2009). Half-precessional dynamics of monsoon rainfall near the East African Equator. *Nature*, *462*(7273), 637-641. https://doi.org/10.1038/nature08520

General rights
It is not permitted to download or to forward/distribute the text or part of it without the consent of the author(s) and/or copyright holder(s), other than for strictly personal, individual use, unless the work is under an open content license (like Creative Commons).

Disclaimer/Complaints regulations
If you believe that digital publication of certain material infringes any of your rights or (privacy) interests, please let the Library know, stating your reasons. In case of a legitimate complaint, the Library will make the material inaccessible and/or remove it from the website. Please Ask the Library: https://uba.uva.nl/en/contact, or a letter to: Library of the University of Amsterdam, Secretariat, P.O. Box 19185, 1000 GD Amsterdam, The Netherlands. You will be contacted as soon as possible.

UvA-DARE is a service provided by the library of the University of Amsterdam (https://dare.uva.nl)

Download date:14 Oct 2026

LETTERS

Half-precessional dynamics of monsoon rainfall near the East African Equator

Dirk Verschuren[1], Jaap S. Sinninghe Damsté[2,3], Jasper Moernaut[4], Iris Kristen[5], Maarten Blaauw[6], Maureen Fagot[1], Gerald H. Haug[7,8] & CHALLACEA project members*

External climate forcings—such as long-term changes in solar insolation—generate different climate responses in tropical and high latitude regions[1]. Documenting the spatial and temporal variability of past climates is therefore critical for understanding how such forcings are translated into regional climate variability. In contrast to the data-rich middle and high latitudes, high-quality climate-proxy records from equatorial regions are relatively few[2–4], especially from regions experiencing the bimodal seasonal rainfall distribution associated with twice-annual passage of the Intertropical Convergence Zone. Here we present a continuous and well-resolved climate-proxy record of hydrological variability during the past 25,000 years from equatorial East Africa. Our results, based on complementary evidence from seismic-reflection stratigraphy and organic biomarker molecules in the sediment record of Lake Challa near Mount Kilimanjaro, reveal that monsoon rainfall in this region varied at half-precessional (~11,500-year) intervals in phase with orbitally controlled insolation forcing. The southeasterly and northeasterly monsoons that advect moisture from the western Indian Ocean were strengthened in alternation when the inter-hemispheric insolation gradient was at a maximum; dry conditions prevailed when neither monsoon was intensified and modest local March or September insolation weakened the rain season that followed. On sub-millennial timescales, the temporal pattern of hydrological change on the East African Equator bears clear high-northern-latitude signatures, but on the orbital timescale it mainly responded to low-latitude insolation forcing. Predominance of low-latitude climate processes in this monsoon region can be attributed to the low-latitude position of its continental regions of surface air flow convergence, and its relative isolation from the Atlantic Ocean, where prominent meridional overturning circulation more tightly couples low-latitude climate regimes to high-latitude boundary conditions.

Mechanistic analyses of past climate change in the tropics have been hampered by the fragmentary or poorly dated nature of palaeoclimate data from key regions; but also by ambiguity about whether low-latitude ocean records are representative of climate history on nearby continents[5], and by the difficulty of extracting independent information on past temperature and precipitation from tropical climate archives (Supplementary Discussion 1). To fill this knowledge gap, we reconstructed the history of rainfall and drought near the Equator in East Africa, using two complementary hydrological proxies extracted from the sediment record of Lake Challa, a crater lake on the lower east slope of Mt Kilimanjaro (3° 19′ S, 37° 42′ E; Supplementary Discussion 2). In this region bordering the western Indian Ocean, the direct climatic influence of Atlantic Ocean circulation is relatively limited, and seasonal migration of tropical convective activity (the Intertropical Convergence Zone, ITCZ) spans the widest latitude range in the world (Fig. 1b). The Challa climate-proxy record can therefore provide unique information on how varying rainfall contributions from the northeasterly (Northern Hemisphere autumn–winter) and southeasterly (Northern Hemisphere spring–summer) monsoons have shaped climate history at the Equator. We find that long-term rainfall variability in equatorial East Africa is a hybrid of patterns typically documented for the northern and southern tropics. The timing of major wet and dry periods over the past 25,000 years has important implications for the nature of ITCZ migration at orbital timescales, and for the cause of glacial-era drought at the Equator.

The moisture-balance history of equatorial East Africa is revealed in seismic-reflection data of Lake Challa's bottom deposits, and the branched and isoprenoid tetraether (BIT) index of soil bacterial versus aquatic archaeal membrane lipids extracted from these sediments (Supplementary Methods 2, 3). Past lake-level fluctuations and events of basin-slope failure recorded by seismic stratigraphy (Fig. 2h) correlate tightly to variations in the water content and lithology of the cored sequence (Supplementary Methods 2). Two older units of inferred lowstand date to the early late-glacial period (L6: ~20,500–14,500 calendar years before present, ~20.5–14.5 cal. kyr BP) and the Younger Dryas (L5: ~12.9–12.0 cal. kyr BP), when most East African lakes are known to have experienced low levels[4]. The four younger, Holocene lowstand units are dated to ~8.0–6.7 (L4), ~5.9–4.7 (L3), ~3.6–3.0 (L2) and ~0.7–0.6 cal. kyr BP (L1). Seismic-reflection evidence for lake-wide mass wasting events or more local basin-slope failures suggest that the lowstand episodes of units L4, L3 and L1 started with abrupt lake-level decline (Supplementary Methods 2). Another mass-wasting event, dated to ~23.4 cal. kyr BP, lacks clear evidence of having been followed by an episode of basin-focused sedimentation, suggesting that a Heinrich-2 (H2) period drought affected equatorial East Africa but was short-lived. The unit of strongly focused sedimentation L6′ represents an extreme lowstand below the mean level of L6, and is dated to ~17.0–16.4 cal. kyr BP, that is, early into the Heinrich-1 (H1) chronozone (Fig. 2h).

The Challa BIT-index record of rainfall-induced surface run-off (Fig. 2g; Supplementary Methods 3) more precisely indicates that post-glacial intensification of the southeasterly Indian Ocean monsoon (driven by increasing summer insolation over North Africa; Fig. 2d) started from 16.5 ± 0.3 cal. kyr BP, and continued into the early

[1]Limnology Unit, Department of Biology, Ghent University, Ledeganckstraat 35, 9000 Gent, Belgium. [2]Faculty of Geosciences, Utrecht University, PO Box 80021, 3508 TA Utrecht, The Netherlands. [3]Department of Marine Organic Biogeochemistry, NIOZ Royal Netherlands Institute for Sea Research, PO Box 59, 1790 AB Den Burg, The Netherlands. [4]Renard Centre of Marine Geology, Department of Geology and Soil Science, Ghent University, Krijgslaan 281 S8, 9000 Gent, Belgium. [5]GeoForschungsZentrum Potsdam, Sektion 3.3 Klimadynamik und Sedimente, Telegrafenberg, D-14473 Potsdam, Germany. [6]School of Geography, Archaeology and Palaeoecology, Queen's University Belfast, BT9 6AX Belfast, UK. [7]Geological Institute, Department of Earth Sciences, ETH Zürich, CH-8092 Zürich, Switzerland. [8]DFG Leibniz Center for Earth Surface Process and Climate Studies, Potsdam University, D-14476 Potsdam, Germany.
*Lists of participants and affiliations appear at the end of the paper.

©2009 Macmillan Publishers Limited. All rights reserved

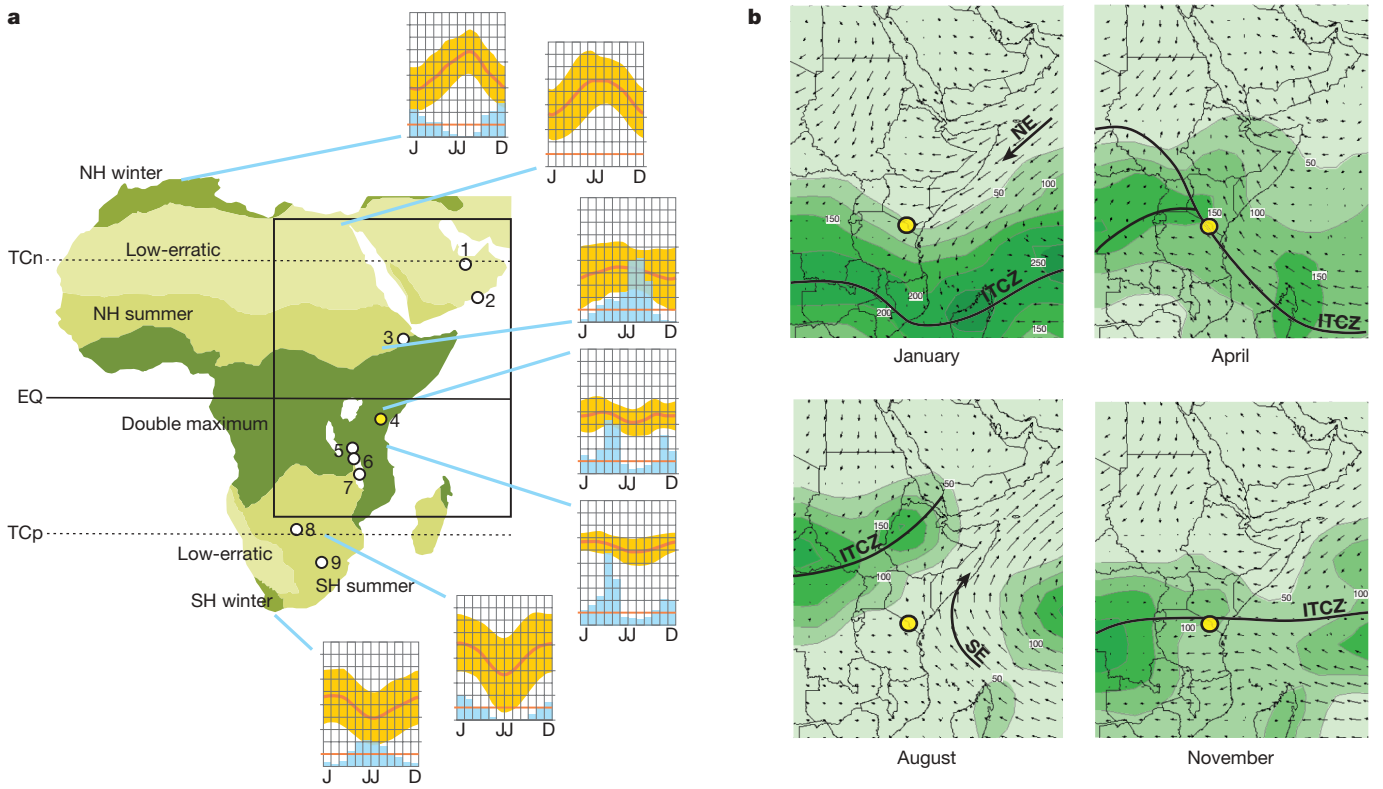

Figure 1 | Location and regional climate of the study site. a, The location of Lake Challa (yellow dot) in relation to the geographical distribution of seasonal rainfall regimes across Africa[4]. Insets, the principal rainfall regimes are illustrated by data on monthly rainfall (January through June/July to December; blue bars at scale intervals of 50 mm) together with the mean and daily range of temperature (red line and ochre shading at scale intervals of 5 °C) at seven representative climate stations; from top to bottom these are Algiers, Cairo, Addis Ababa, Nairobi, Dar Es Salaam, Gantsi and Cape Town. Numbered sites (1–9) refer to continental palaeodata in a latitudinal transect mostly bordering the western Indian Ocean, identified in Supplementary Fig. 5. NH, Northern Hemisphere; SH, Southern Hemisphere. EQ, Equator; TCn, Tropic of Cancer; TCp, Tropic of Capricorn. Boxed area shown magnified in **b**. **b**, Synoptic climatology of tropical East Africa for four representative months. The panels show the seasonal migration of the Intertropical Convergence Zone (ITCZ) and associated rain belts across the study region. Monthly precipitation (shaded green, with contours at 50 mm intervals) is based on gauge data over land, and satellite estimates over sea. Also indicated are wind fields for the 925 hPa pressure level (arrows), with wind speed proportional to arrow length (http://iridl.ldeo.columbia.edu).

Holocene, interrupted only by severe Younger Dryas aridity. Thus, monsoon circulation on the East African Equator started to intensify ~1,700 years before the Indian (that is, South Asian) and East Asian monsoons did so (at 14.8 cal. kyr BP: refs 6, 7 and Fig. 2c). The Asian monsoons are believed to have responded late to insolation forcing because the Arctic sea-ice expansion which cooled northern Eurasia during H1 initially weakened monsoonal moisture advection from the Indian and western Pacific oceans into southern Eurasia[8]. Also in the tropical Atlantic Ocean, H1-period slowdown of the meridional overturning circulation[9] and presumed southward shift of the ITCZ[10] delayed post-glacial strengthening of the West African monsoon to ~15 cal. kyr BP[11]. For East African regions receiving rainfall exclusively from the Indian Ocean, neither the source region of moist air (the southern Indian Ocean) nor its continental destination of surface flow convergence (the North African land mass) were strongly affected by H1 cooling[10], so moisture advection intensified as soon as enhanced Northern Hemisphere summer insolation created a sufficient land–sea temperature contrast between them[12]. Considering that tropical wetlands were the probable source of early late-glacial (pre-14.8 cal. kyr BP) CH_4 changes (Supplementary Discussion 3), eastern equatorial Africa must have been among those regions contributing to the rise in atmospheric CH_4 just before and during H1 (Fig. 2a). Throughout the Northern Hemisphere tropics, triggering of strong monsoon circulation was delayed pending favourable land and ocean thermal conditions, which initially remained under the control of climate events in the North Atlantic Ocean (Supplementary Discussion 4).

Our Challa BIT record further shows that drought encompassing the Younger Dryas in equatorial East Africa lasted from 13.3 to 11.7 cal. kyr BP, with most intense aridity during 12.4–12.8 cal. kyr BP, and that at the start of the Holocene the southeasterly monsoon regained its full strength in less than 200 years (Fig. 2g). Within dating error, this end to Younger Dryas drought in East Africa is coeval with corresponding signatures in records of the Indian[7], East Asian (ref. 6 and Fig. 2c), and tropical Atlantic monsoons[13], testifying to the rapid reorganization of low-latitude atmospheric circulation patterns following abrupt warming in the northern North Atlantic (Fig. 2b). Rapid resumption of ITCZ migration far into the Northern Hemisphere is also indicated by the abruptly intensifying southerly winds at ~11.7 cal. kyr BP across southern equatorial Africa (ref. 14 and Supplementary Discussion 5). The end of African Younger Dryas drought at Challa matches the tentative age assigned to the base of the current ice cap on Mt Kilimanjaro[15]. It thus appears that Mt Kilimanjaro's glacial-era ice cap (Supplementary Discussion 6), possibly in retreat since the start of regional post-glacial warming ~20 cal. kyr BP[16], was finally eradicated by severe Younger Dryas drought.

In its entirety, the 25,000-year Challa BIT record (Fig. 2g) implies relatively moist conditions in equatorial East Africa during the periods >25–20.5 (H2 excluded), 14.5–8.5 (the Younger Dryas excluded) and since 4.5 cal. kyr BP; and relative drought during the periods 20–16.5 and 8.5–4.5 cal. kyr BP. The Holocene part of this moisture-balance history differs markedly from that of sites in either northern tropical Africa, or southeastern tropical Africa from ~9° S (Supplementary Discussion 7). Today those regions experience a unimodal seasonal distribution of monsoon rainfall (Fig. 1a) in which the single wet season occurs during peak summer insolation over the corresponding hemisphere; and, like monsoon systems elsewhere[6,17,18], their long-term history reflects (more or less gradual) variation in monsoon strength that is controlled by precession-driven variation in Northern or

©2009 Macmillan Publishers Limited. All rights reserved

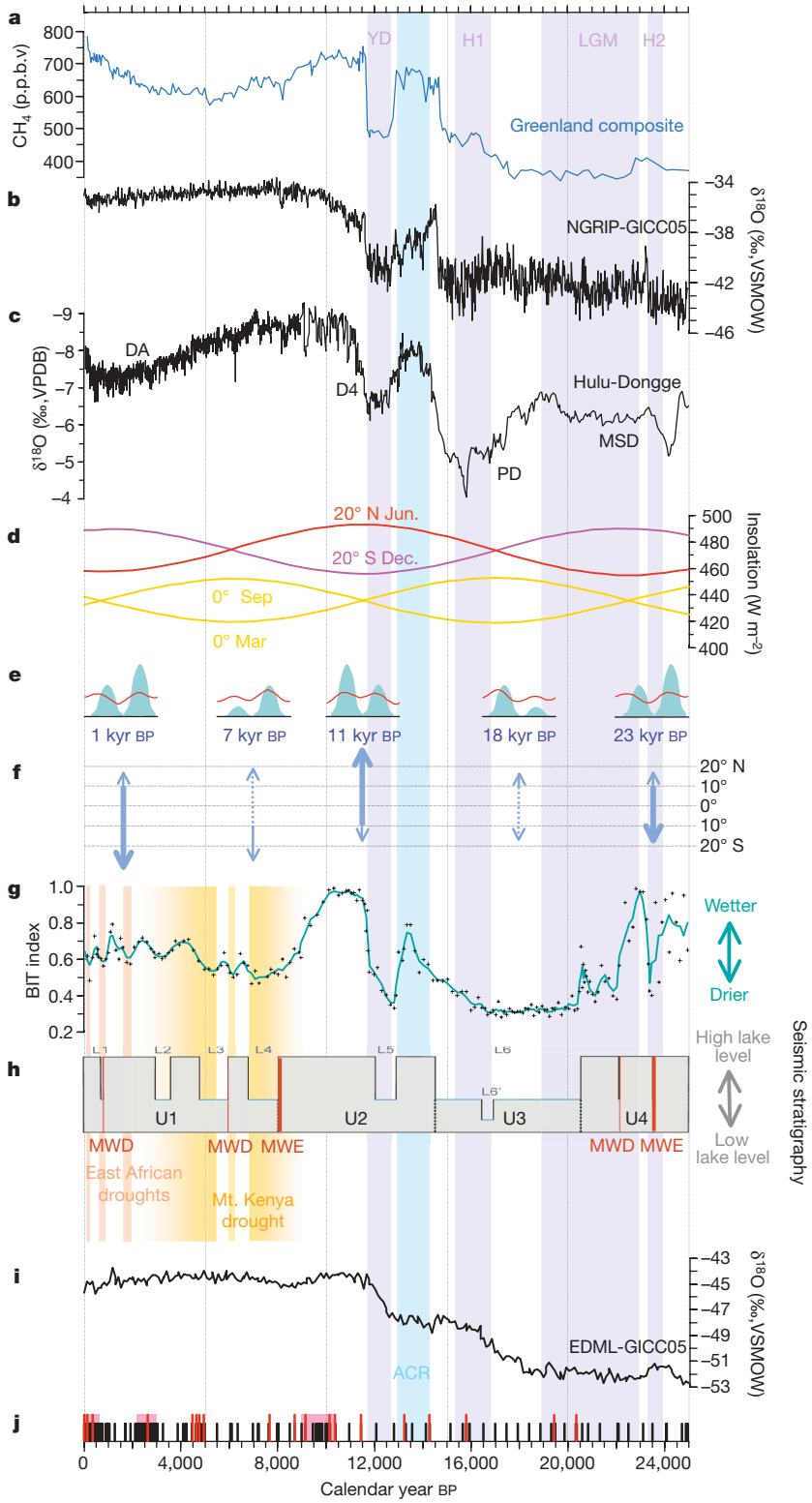

Figure 2 | Lake Challa climate-proxy data in context. Comparison of Lake Challa data (**g**, **h**) with selected other climate records (**a**–**c**, **i**), insolation (**d**) and schematic rainfall parameters (**e**, **f**). Relevant chronozones are shaded in purple and blue for northern and southern high-latitude influences respectively, and orange/pink for regional Holocene droughts. YD, Younger Dryas; ACR, Antarctic Cold Reversal; H1 and H2, Heinrich events 1 and 2; LGM, Last Glacial Maximum. **a**, Greenland composite (NGRIP-GISP2-GRIP) atmospheric CH_4 record[28]. **b**, Greenland (NGRIP) ice core $\delta^{18}O$ on the GICC05 timescale (ref. 29). **c**, Hulu/Dongge cave stalagmite $\delta^{18}O$ (ref. 6 and references therein); D4, DA, PD and MSD are the individual stalagmite samples making up this composite record. **d**, June and December insolation at 20° N/S, and March and September insolation on the Equator[30]. **e**, Monthly insolation[30] and schematic representation of seasonal rainfall in the Lake Challa region (January through December) at 1, 7, 11, 18 and 23 kyr BP, illustrating the joint effects on total annual rainfall of (1) a strengthened monsoon associated with a peak summer/winter insolation contrast between the hemispheres (which increases rainfall during either the long or short rain season) and (2) variation in local March or September insolation (with modest maxima causing the ensuing rain season to wither). **f**, Schematic representation of the approximate latitudinal extent of ITCZ migration in the western Indian Ocean at 1, 7, 11, 18 and 23 kyr BP, under the combined influence of low-latitude insolation forcing and (during glacial time) the equatorward displacement of the southern polar front; the line thickness of upward and downward arrows is proportional to the relative intensity of the southeasterly and northeasterly monsoons, respectively. **g**, Challa BIT-index rainfall reconstruction, individual data with three-point moving average. **h**, Challa lake-level reconstruction based on seismic-reflection stratigraphy (Supplementary Methods 1, 3). U1–U4, seismic units; L1–L6 and L6′, lowstand episodes; red marker horizons, basin-wide mass-wasting events (MWEs) and more local mass-wasting deposits (MWDs). **i**, Antarctica EDML ice core $\delta^{18}O$ record on the NGRIP-GICC05 timescale[28]. **j**, The Challa age–depth model (Supplementary Fig. 3) is derived from AMS ^{14}C dates on bulk organic carbon (black tick marks), corrected for an evolving lake-carbon reservoir age between 200 and 450 years determined at 19 depth intervals (red tick marks); the pink areas indicate sections of successful wiggle-match dating (Supplementary Methods 2).

Southern Hemisphere summer insolation (Fig. 2d). In equatorial East Africa, twice-yearly passing of ITCZ-associated rain belts (Fig. 1b) produces a bimodal seasonal rainfall pattern (Fig. 1a and Supplementary Discussion 2), and hence predicts a doubled frequency of precession-driven wet and dry periods as the southeasterly and northeasterly monsoons are enhanced in alternation. Clear manifestation of such 'double-frequency' (that is, ~11,500-year interval) wet–dry cycles in a palaeorecord may partly depend on the local prominence of dry seasons, as is the case in semi-arid southeastern Kenya (Supplementary Discussion 2). Over the past 25,000 years, equatorial East Africa experienced high rainfall when early-summer insolation peaked in either the northern or the southern tropics (that is, at ~22.5, 11.5 and 1.5 kyr BP; Fig. 2g, d), the summer/winter inter-hemispheric insolation gradient was large, and either the southeasterly or northeasterly monsoon was intensified[19]. Rainfall was reduced when the summer/winter inter-hemispheric insolation gradient was modest (at 17–18 and 6–7 kyr BP), and neither monsoon was particularly intensified (Supplementary Discussion 8). From an equatorial perspective, drought at those times may also have resulted because the coincident minimum in local insolation[20] during September (17–18 kyr BP) or March (6–7 kyr BP) caused the rain season which followed it to fail or wither (Fig. 2e and Supplementary Discussion 9).

©2009 Macmillan Publishers Limited. All rights reserved

Focusing on the Holocene, the Challa pattern of a short early-Holocene humid period followed first by mid-Holocene drought and then wetter late-Holocene conditions (Fig. 2g, h) has also been recorded at other African lakes located between the Equator and ~8° S (Supplementary Discussion 7). Based on palaeovegetation data, Peyron *et al.*[21] located the transition area between a wetter (northern tropical) and drier (southern tropical) mid-Holocene climate regime between the Equator and 3° S, that is, just north of Lake Challa. Alternation of wet and dry climate at a half-precessional interval is also evident in the early part of the Challa BIT record, as local glacial drought was limited to a ~4,000-year period between 20.5 and 16.5 cal. kyr BP (Fig. 2g). That in eastern (but not western) tropical Africa this 'Last Glacial Maximum (LGM) drought' was immediately preceded by a wet phase is well-documented[4]. Recently it has been recognized that in some regions of southeastern tropical Africa even the LGM was not particularly dry[22,23]. Importantly, we can establish that peak glacial drought in equatorial East Africa overlapped only partly with the LGM proper (Fig. 2g and Supplementary Discussion 10). For most of its duration it instead coincided with a modest summer/winter inter-hemispheric insolation contrast (Fig. 2d), as was the case during the mid-Holocene dry period.

Following mid-Holocene drought, rainfall in equatorial East Africa increased again from ~6.8 cal. kyr BP (peaking between 4.5 and 2 cal. kyr BP), but was modulated by distinct multi-century droughts (Fig. 2g). The double-peaked wet period at ~6.8–5.5 cal. kyr BP, which interrupts mid-Holocene drought in the BIT record and is represented in seismic stratigraphy by the inferred highstand separating L4 and L3 (Fig. 2h), matches the timing of a similarly double-peaked wet period interrupting mid-Holocene drought on Mt Kenya (ref. 24 and Supplementary Discussion 11). Further, the three most prominent dry episodes of the last two millennia recorded at Challa (2.0–1.6, 0.8–0.6 and 0.2–0.15 cal. kyr BP) match the timing of droughts known to have had broad regional impact in continental East Africa (ref. 25 and Supplementary Discussion 12). In summary, our Challa BIT data are also consistent with available regional palaeohydrological information at multi-decadal to century timescales. Notwithstanding our monitoring of the modern system (see Supplementary Methods 3), uncertainty remains regarding the exact process by which branched and isoprenoid tetraether lipids are transferred to and incorporated in Lake Challa sediments, and hence, about the precise relationship of the Challa BIT index to past rainfall variation in the Challa region at the multi-decadal resolution of our reconstruction. Our confidence in the truthfulness of the Challa BIT index as a hydrological proxy is based partly on its excellent agreement both with the (lower-resolution) Challa seismic-stratigraphic record of past lake-level fluctuations, and with diverse other high-quality palaeohydrological indicators from equatorial East Africa at a wide range of timescales (Figs 2g and Supplementary Fig. 7). The unique combination of adequate time coverage (25,000 years) and high resolution presented by the Challa BIT climate-proxy record, together with the long-term stability of the Challa sedimentary environment (Supplementary Discussion 2), are key to the climate-dynamical insights generated.

In regions bordering the western Indian Ocean, opposite Holocene moisture-balance trends were established in the northern and southern tropics, and a hybrid pattern near the Equator, from immediately after the Younger Dryas (Supplementary Discussion 7). The early end of the African humid period[11] near the Equator contrasts with its persistence until ~6.0–5.0 cal. kyr BP in northeastern tropical Africa, related to Northern Hemisphere summer insolation control on Indian monsoon intensity[7]. During the LGM and the deglaciation period, northern ice-sheet influence and reduced Indian Ocean sea surface temperatures partly overrode low-latitude insolation influence on monsoon intensity and evaporation, creating more cross-equatorial uniformity in moisture-balance trends. Southeastern Africa enjoyed greater moisture than other tropical regions during the LGM proper, partly because of modest (1.5–2.0 °C) glacial cooling of the tropical Indian Ocean[26]. Also, the southern mid-latitude cooling associated with expanded circum-Antarctic sea ice impeded southward movement of the ITCZ during Southern Hemisphere summer (Fig. 2f), thereby compressing the tropical convective zone to a narrower latitudinal band[4]. These processes worked together with the orbitally enhanced northeasterly monsoon to break LGM-era drought in southeastern tropical Africa. They may also explain the high rainfall in equatorial East Africa immediately before and halfway into the LGM (Fig. 2g). Our equatorial data thus highlight the notion that orbital-scale ITCZ 'migration', or shifts in its mean annual latitudinal position, mainly relates to variation in how far high-latitude influences on lower mid-latitude climate allowed the ITCZ to move into the northern or southern hemisphere during summer (Fig. 2f); the cross-equatorial position of the region with twice-annual ITCZ passage, and hence bimodal rainfall regime, was probably not much affected (Supplementary Discussion 13).

The distinct timing of late-glacial drought on the Equator (20.5–16.5 cal. kyr BP) does not fit well with Northern Hemisphere glaciation being its primary driver. It is best attributed to partial failure of the short rain season due to modest local September insolation, perhaps exacerbated by weakening of the southeasterly monsoon due to northern cooling modestly affecting the North African land mass. Following establishment of interglacial temperatures (by 11.5 cal. kyr BP; ref. 16), low-latitude insolation clearly became the dominant driver of regional moisture balance, with strong north–south anti-phasing across the Equator revealing the signature of orbital precession[27].

On balance, low-latitude orbital forcing has exerted a dominant influence on climate in the western Indian Ocean throughout the past 25,000 years, including the LGM and deglaciation periods. High-latitude influences challenged this primacy only during the Younger Dryas, Heinrich events (to lesser extent), and perhaps also during some of the multi-century droughts that punctuated the relatively moist late Holocene (Fig. 2g and Supplementary Discussion 12). Important keys to the near-continuous prominence of low-latitude climate processes in this monsoon region are the low-latitude position of its continental regions of surface air flow convergence (in contrast to those of the Indian and East Asian monsoons) and its relative isolation from the Atlantic Ocean domain, where important latitudinal heat redistribution by the meridional overturning circulation more tightly coupled tropical climate history to high-latitude boundary conditions.

METHODS SUMMARY

A dense grid of echo-sounding and very-high-resolution seismic reflection profiles was acquired in 2003 using a 3.5 kHz Geopulse system. In 2003 and 2005 we recovered from a mid-lake location (Supplementary Fig. 1) gravity cores with intact sediment–water interface, a mini-Kullenberg piston core of 2.6 m length and three parallel UWITEC hammer-driven piston cores of 22 m. After cross-correlation of successive overlapping core sections, and excision of five turbidites (42, 36, 5, 6 and 14 cm thick) that consist largely of re-deposited crater slope material, the recovered sediment profile constituted a continuous, 20.82-m-long composite sequence of mostly finely laminated organic muds rich in diatom silica. Seismic-stratigraphic signatures of past lake-level fluctuation and mass-wasting events were linked to the lithology of the cored sediment sequence at the level of turbidites with clear seismic signature, and through patterns in sediment water content. The cored sediment sequence was dated using AMS ^{14}C dates on bulk organic carbon, corrected for an evolving lake-carbon reservoir age through combination with ^{210}Pb-dated sub-recent sediments, AMS ^{14}C dates on grass charcoal, and wiggle-match dating (Supplementary Methods 2).

For organic geochemistry, powdered and freeze-dried sediments (1–3 g dry mass) were extracted by Dionex accelerated solvent extraction with 9:1 dichloromethane/methanol by volume. The extracts were separated by Al_2O_3 column chromatography with 9:1 hexane/dichloromethane and 1:1 dichloromethane/methanol. The polar fraction was condensed by rotary evaporation, dissolved in 99:1 hexane/isopropanol, and filtered using a PTFE 0.4 μm filter before analysis of tetraether lipids by high-performance liquid chromatography/atmospheric-pressure chemical ionization mass spectrometry (HPLC/APCI-MS). Glycerol dialkyl glycerol tetraether lipids were detected by single ion monitoring of their $[M+H]^+$ ions

©2009 Macmillan Publishers Limited. All rights reserved

(dwell time 234 ms), quantified by integration of peak areas, and used to calculate the BIT index (Supplementary Methods 3). All BIT analyses were run in duplicate; average error is <0.01 unit.

Received 10 January; accepted 15 September 2009.

1. Clement, A. C., Hall, A. & Broccoli, A. J. The importance of precessional signals in the tropical climate. *Clim. Dyn.* **22,** 327–341 (2004).
2. Partin, J. W., Cobb, K. M., Adkins, J. F., Clark, B. & Fernandez, D. P. Millennial-scale trends in west Pacific warm pool hydrology since the Last Glacial Maximum. *Nature* **449,** 452–455 (2007).
3. Cruz, F. W. *et al.* Orbitally driven east-west antiphasing of South American precipitation. *Nature Geosci.* **2,** 210–214 (2009).
4. Gasse, F., Chalié, F., Vincens, A., Williams, M. A. J. & Williamson, D. Climatic patterns in equatorial and southern Africa from 30,000 to 10,000 years ago reconstructed from terrestrial and near-shore proxy data. *Quat. Sci. Rev.* **27,** 2316–2340 (2008).
5. Trauth, M. H., Maslin, M. A., Deino, A. & Strecker, M. R. Late Cenozoic moisture history of East Africa. *Science* **309,** 2051–2053 (2005).
6. Wang, Y. J. *et al.* Millennial- and orbital-scale changes in the East Asian monsoon over the past 224,000 years. *Nature* **451,** 1090–1093 (2008).
7. Fleitmann, D. *et al.* Holocene ITCZ and Indian monsoon dynamics recorded in stalagmites from Oman and Yemen (Socotra). *Quat. Sci. Rev.* **26,** 170–188 (2007).
8. Vellinga, M. & Wood, R. A. Global climatic impacts of a collapse of the Atlantic thermohaline circulation. *Clim. Change* **54,** 251–267 (2002).
9. McManus, J. F., Francois, R., Gherardi, J. M., Keigwin, L. D. & Brown-Leger, S. Collapse and rapid resumption of Atlantic meridional circulation linked to deglacial climate changes. *Nature* **428,** 834–837 (2004).
10. Zhang, R. & Delworth, T. L. Simulated tropical response to a substantial weakening of the Atlantic thermohaline circulation. *J. Clim.* **18,** 1853–1860 (2005).
11. deMenocal, P. *et al.* Abrupt onset and termination of the African Humid Period: rapid climate responses to gradual insolation forcing. *Quat. Sci. Rev.* **19,** 347–361 (2000).
12. Kutzbach, J. E. Monsoon climate of the early Holocene: climate experiment with Earth's orbital parameters for 9000 years ago. *Science* **214,** 59–61 (1981).
13. Peterson, L. C., Haug, G. H., Hughen, K. A. & Röhl, U. Rapid changes in the hydrological cycle of the tropical Atlantic during the last glacial. *Science* **290,** 1947–1950 (2000).
14. Talbot, M. R., Filippi, M. L., Jensen, N. B. & Tiercelin, J.-J. An abrupt change in the African monsoon at the end of the Younger Dryas. *Geochem. Geophys. Geosyst.* **8,** doi:10.1029/2006GC001465 (2007).
15. Thompson, L. G. *et al.* Kilimanjaro ice core records: evidence of Holocene climate change in tropical Africa. *Science* **298,** 589–593 (2002).
16. Tierney, J. E. *et al.* Northern Hemisphere controls on tropical Southeast African climate during the last 60,000 years. *Science* **322,** 252–255 (2008).
17. Cruz, F. W. *et al.* Insolation-driven changes in atmospheric circulation over the past 116,000 years in sub-tropical Brazil. *Nature* **434,** 63–66 (2005).
18. Haug, G. H., Hughen, K. A., Sigman, D. M., Peterson, L. C. & Rohl, U. Southward migration of the intertropical convergence zone through the Holocene. *Science* **293,** 1304–1308 (2001).
19. Thevenon, F., Williamson, D. & Taieb, M. A 22-kyr BP sedimentological record of Lake Rukwa (8° S, SW Tanzania): environmental, chronostratigraphic and climatic implications. *Palaeogeogr. Palaeoclimatol. Palaeoecol.* **187,** 285–294 (2002).
20. Berger, A., Loutre, M. F. & Mélice, J. L. Equatorial insolation: from precession harmonics to eccentricity frequencies. *Clim. Past* **2,** 131–136 (2006).
21. Peyron, O., Jolly, D., Bonnefille, R., Vincens, A. & Guiot, J. Climate of East Africa 6000 ^{14}C yr BP as inferred from pollen data. *Quat. Res.* **54,** 90–101 (2000).
22. Garcin, Y., Vincens, A., Williamson, D., Guiot, J. & Buchet, G. Wet phases in tropical southern Africa during the last glacial period. *Geophys. Res. Lett.* **33,** L07703, doi:10.1029/2005GL025531 (2006).
23. Mumbi, C. T., Marchant, R., Hooghiemstra, H. & Wooller, M. J. Late Quaternary vegetation reconstruction from the Eastern Arc Mountains, Tanzania. *Quat. Res.* **69,** 326–341 (2008).
24. Barker, P. A. *et al.* A 14,000-year oxygen isotope record from diatom silica in two alpine lakes on Mt. Kenya. *Science* **292,** 2307–2310 (2001).
25. Verschuren, D. & Charman, D. J. in *Natural Climate Variability and Global Warming* (eds Battarbee, R. W. & Binney, H. E.) 189–231 (Wiley-Blackwell, 2008).
26. Pinot, S. *et al.* Tropical paleoclimates at the Last Glacial Maximum: comparison of Paleoclimate Modeling Intercomparison Project (PMIP) simulations and paleodata. *Clim. Dyn.* **15,** 857–874 (1999).
27. Ruddiman, W. F. What is the timing of orbital-scale monsoon changes? *Quat. Sci. Rev.* **25,** 657–658 (2006).
28. EPICA community members.. One-to-one coupling of glacial climate variability in Greenland and Antarctica. *Nature* **444,** 195–198 (2006).
29. Rasmussen, S. O. *et al.* A new Greenland ice core chronology for the last glacial termination. *J. Geophys. Res.* **111,** doi:10.1029/2005JD006079 (2006).
30. Berger, A. & Loutre, M.-F. Insolation values for the climate of the last 10 million years. *Quat. Sci. Rev.* **10,** 297–317 (1991).

Supplementary Information is linked to the online version of the paper at www.nature.com/nature.

Acknowledgements This research was sponsored by funding agencies in Belgium (FWO-Vlaanderen), Denmark (Danish National Research Council), Germany (DFG) and The Netherlands (NWO) through the European Science Foundation (ESF) EuroCORES programme, EuroCLIMATE. Fieldwork was conducted with permission of the Kenyan Ministry of Education, Science and Technology (MOEST) and the Tanzania Commission for Science and Technology (COSTECH). We thank A. Alcantara, M. Kohler, S. Lauterbach, R. Niederreiter and S. Opitz for assistance with core collection and processing; D. Engstrom for ^{210}Pb dating, A. Berger, D. Fleitmann, J. Kutzbach and Z. Liu for discussion, and E. Odada for support. J.M. acknowledges the support of the Institute for the Promotion of Innovation through Science and Technology in Flanders (IWT-Vlaanderen).

Author Contributions D.V. initiated and coordinated the research, and wrote the paper. J.S.S.D. was responsible for the production of the biomarker data, J.M. interpreted the seismic-reflection data, I.K. constructed the composite sediment sequence and depth scale, M.B. developed the sediment age model, and M.F. supervised core sampling and managed the project database. G.H.H. and all CHALLACEA members contributed their expertise to improving the discussed data sets and/or the manuscript.

Author Information Reprints and permissions information is available at www.nature.com/reprints. Correspondence and requests for materials should be addressed to D.V. (dirk.verschuren@UGent.be).

CHALLACEA project members Bas van Geel[1], Marc De Batist[2], Philip Barker[3], Mathias Vuille[4], Daniel J. Conley[5], Daniel O. Olago[6], Isla Milne[7], Birgit Plessen[8], Hilde Eggermont[9], Christian Wolff[8], Elizabeth Hurrell[3], Jort Ossebaar[10], Anna Lyaruu[1], Johannes van der Plicht[11], Brian F. Cumming[7], Achim Brauer[8], Stephen M. Rucina[12], James M. Russell[13], Edward Keppens[14], Joseph Hus[15], Raymond S. Bradley[16], Melanie Leng[17], Jens Mingram[8] & Norbert R. Nowaczyk[8]

[1]Institute for Biodiversity and Ecosystem Dynamics, Research Group Paleoecology and Landscape Ecology, Faculty of Science, Universiteit van Amsterdam, 1098 SM Amsterdam, The Netherlands. [2]Renard Centre of Marine Geology, Department of Geology and Soil Science, Ghent University, Krijgslaan 281 S8, 9000 Gent, Belgium. [3]Lancaster Environment Centre, Lancaster University, Lancaster LA1 4YQ, UK. [4]Atmospheric and Environmental Sciences, State University of New York, Albany, New York 12222, USA. [5]GeoBiosphere Centre, Department of Geology, Lund University, SE-223 62 Lund, Sweden. [6]Department of Geology, University of Nairobi, PO Box 30197, Nairobi, Kenya. [7]Paleoecological Environmental Assessment and Research Laboratory, Department of Biology, Queen's University, Kingston, ON K7L 3N6, Canada. [8]GeoForschungsZentrum Potsdam, Sektion 3.3 Klimadynamik und Sedimente, Telegrafenberg, D-14473 Potsdam, Germany. [9]Limnology Unit, Department of Biology, Ghent University, Ledeganckstraat 35, 9000 Gent, Belgium. [10]Faculty of Geosciences, Utrecht University, PO Box 80021, 3508 TA Utrecht, The Netherlands. [11]Center for Isotope Research, Groningen University, 9747 AG Groningen, The Netherlands. [12]Department of Palynology, National Museums of Kenya, Museum Hill, Nairobi, Kenya. [13]Geological Sciences, Brown University, Providence, Rhode Island 02912, USA. [14]Department of Geology, Vrije Universiteit Brussel, Pleinlaan 2, B-1050 Brussels, Belgium. [15]Centre de Physique du Globe, Royal Meteorological Institute, 5670 Dourbes, Belgium. [16]Climate System Research Center, Department of Geosciences, University of Massachusetts, Amherst, Massachusetts 01003-9297, USA. [17]NERC Isotope Geosciences Laboratory, British Geological Survey, Keyworth, Nottingham NG12 5GG, UK.

©2009 Macmillan Publishers Limited. All rights reserved